

# Wetting and interactions of Ag–Cu–Ti and Ag–Cu–Ni alloys with ceramic and steel substrates for use as sealing materials in a DCFC stack

G. Triantafyllou<sup>1</sup> · J. T. S. Irvine<sup>1</sup>

Received: 9 July 2015 / Accepted: 23 October 2015 / Published online: 5 November 2015  
© The Author(s) 2015. This article is published with open access at Springerlink.com

**Abstract** Ag and Ag-based pseudo-alloys were evaluated in terms of application as metal brazes for the use in a hybrid direct carbon fuel cell stack. This paper reports on a series of wetting experiments on systems of pure Ag as well as Ag–Cu–Ti and Ag–Cu–Ni pseudo-alloys in contact with the widely used austenitic stainless steel SS316L, the ferritic steels Crofer22APU and Crofer22H and with polycrystalline partially stabilized zirconia (TZ-3Y) for the determination of the interfacial properties of the above systems. Pure Ag in air showed poor wettability ( $\theta > 90^\circ$ ) with all substrates. The Ag–Cu–Ti pseudo-alloy in vacuum ( $P = 2.5 \times 10^{-3}$  mbar) showed improved wettability, with  $\theta \approx 40^\circ$  for the steels and  $\theta \approx 50^\circ$  for the TZ-3Y substrates. The Ag–Cu–Ni pseudo-alloy in air showed excellent wetting properties ( $\theta < 10^\circ$ ) with all the substrates, but its high liquidus temperature makes it unsuitable for use with the SS316L steel. In low vacuum ( $P = 1.5 \times 10^{-1}$  mbar), the contact angle was increased ( $\theta \approx 65^\circ$ ) but the low oxygen concentration limits the oxidation of the steel surface. Selected systems of the pseudo-alloys in contact with steel and TZ-3Y substrates were treated for 120 h in the operating conditions of a hybrid direct carbon fuel cell, in order to evaluate the thermal stability of the joints. Despite the reactions taking place on the interface, the joints showed good stability and no separation of the two phases occurred.

## Introduction

A direct carbon fuel cell (DCFC) converts the chemical energy stored in a carbon-rich material to electricity through its direct electrochemical oxidation. Direct conversion of coal to electricity offers significant increase in efficiency with consequent reductions in CO<sub>2</sub> emissions [1]. A hybrid direct carbon fuel cell (HDCFC) combines the advantages of a molten carbonate fuel cell (MCFC) and a solid oxide fuel cell (SOFC) and uses a hybrid-state (molten-solid) design, in order to increase the overall performance of the cell [2]. Sealing materials play a crucial role in the performance and long-term durability of a DCFC stack, as they minimize gas leakage and ensure the thermomechanical stability and the fuel purity.

Two different types of high-temperature sealing materials are widely used. Electronic conductive sealants, usually noble metals, for use in the interconnects and current collectors interfaces and non-electronic conductive sealants, normally silicate-based glass materials, in order to electrical insulate the individual cells of the stack [3]. One common problem of those glass sealants is the devitrification that occurs during the long-term thermal treatment of the glasses and affects their thermomechanical stability, leading to more fragile structures [4, 5]. However, recent studies showed that the employment of an electrical insulation layer on the steel components makes possible the use of a single metal braze sealant in all parts of the stack [6].

The joining of the stack components requires the formation of strong bonds on the filler metal—stainless steel and ceramic (insulating layer) interfaces. The rapid heating rates and the high-operating temperatures ( $\sim 1023$  K) of the DCFC can lead to increased stress on the joining and sealing points of the stainless steel components of the stack [7]. Also, the stainless steel body parts as well as the

✉ G. Triantafyllou  
gt42@st-andrews.ac.uk

J. T. S. Irvine  
jtsi@st-andrews.ac.uk

<sup>1</sup> School of Chemistry, University of St Andrews, St Andrews, Scotland, UK

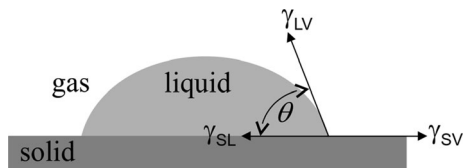


**Fig. 1** Schematic profile of a contact angle,  $\theta$ , in a solid–liquid–vapour system, in equilibrium

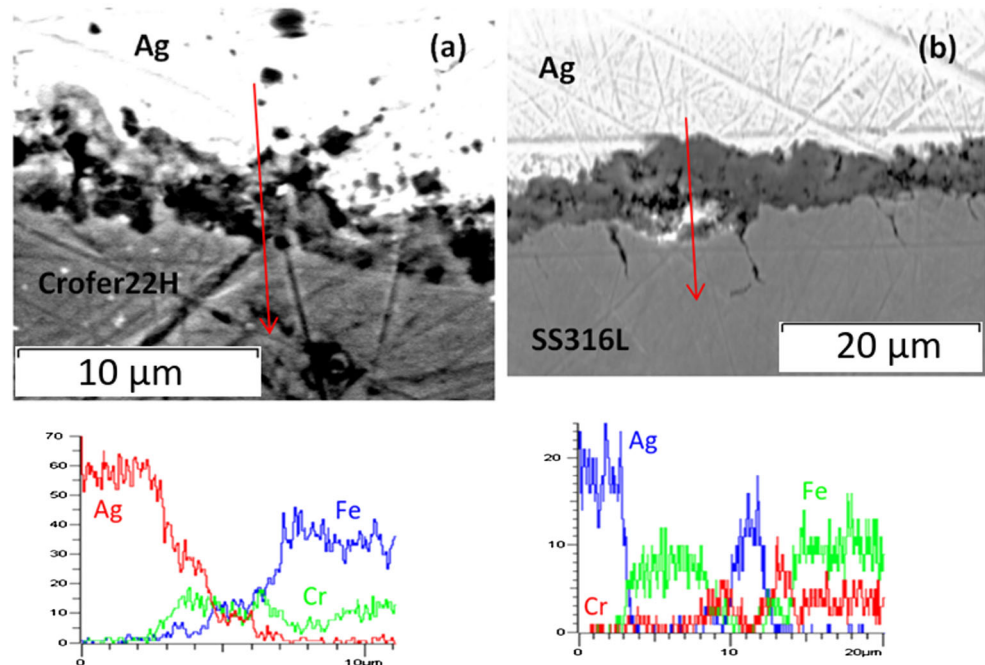
**Table 1** Chemical composition (%max) for SS316L, Crofer22APU and Crofer22H

Steel	Cr	C	Mn	Si	Cu	Al	S	P
SS316L	18	0.03	2.00	0.75			0.03	0.045
Crofer22APU	24	0.03	0.80	0.50	0.50	0.50	0.020	0.05
Crofer22H	24	0.03	0.80	0.60	0.50	0.10	0.006	0.05
Steel	Ti	La	N	W	Nb	Ni	Mo	Fe
SS316L			0.10			14	3.00	bal
Crofer22APU	0.20	0.20						
Crofer22H	0.20	0.20	0.03	3.0	1.0			

**Table 2** Temperature dependence of the contact angles,  $\theta$  ( $^{\circ}$ ), for the systems of Ag in contact with steels and TZ-3Y in air

$T$ (K)	SS316L/ Ag	Crofer22APU/ Ag	Crofer22H/ Ag	TZ-3Y/ Ag
1253	92.7	92.6	110.9	107.7
1293	91.4	90.5	109.5	108.8
1333	90.0	89.8	108.1	109.1
1373	89.4	89.2	106.6	109.8

**Fig. 2** Cross section SEM-EDX line scanning analysis on the interface of Crofer22H/CuO/Ag (a) and SS316L/CuO/Ag (b) samples after wetting experiment at  $T = 1253$  K, in air



sealing and insulating materials must be resistant to corrosion and to be able to cope with thermal cycles as well as with long term operation in high temperatures. Ag is an excellent candidate for filler metal because of its high stability against oxidation in high temperature, high mechanical strength, good electrical and thermal conductivity and its reasonable cost. Contact angle ( $\theta$ ) is another important factor in sealing. Low values of contact angles are crucial in order to ensure good stability and strong interfacial bond between the contacting phases. One disadvantage of using pure Ag is the poor wettability of liquid



**Fig. 3** Separation of the Ag drop from the SS316L/Cu substrate, after wetting experiment in air. The Fe–O layer formed on the surface of the steel can be found on the Ag drop

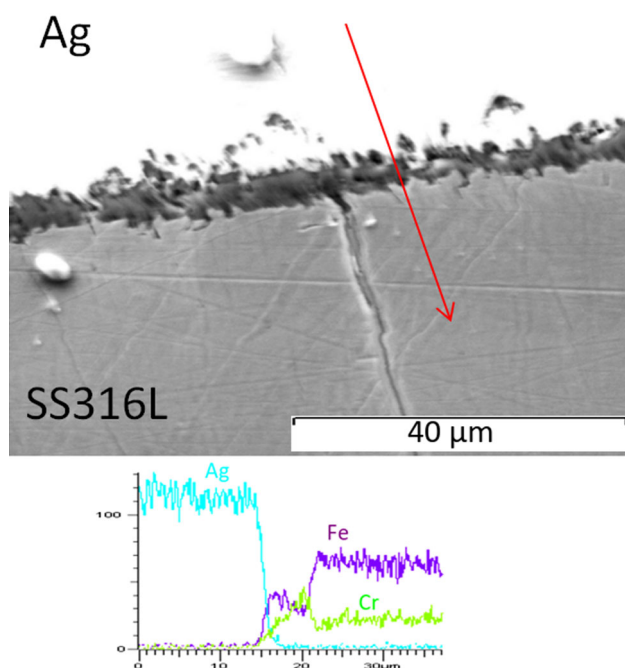


**Fig. 4** Cross section SEM-EDX analysis on the interface of a SS316L/Ti/CuO/Ag sample after wetting experiment at  $T = 1253$  K, in air

Ag in contact with steel and ceramic substrates. Literature data for wetting experiments on liquid Ag/ceramic oxides systems show very bad wetting ( $\theta > 120^\circ$ ) for low values of oxygen partial pressure [8, 9]. Because of the high diffusivity and solubility of oxygen in liquid Ag, the surface energy of liquid Ag drops significantly in air. This causes a parallel drop in the contact angles values of Ag in contact with ceramic oxides, but the systems remain non-wetting ( $\theta > 90^\circ$ ) [10, 11]. In the case of the wetting of the stainless steels, a Cr–O-rich protective layer is formed in the surface of the steel and the liquid metal phase is in contact with this ceramic phase, making the wetting experiment a liquid Ag/ceramic oxide wetting.

In order to improve the wetting properties of pure Ag, some Ag-based alloys have been developed. Two commonly used alloys are the (wt.%)  $\text{Ag}_{63}\text{Cu}_{35.25}\text{Ti}_{1.75}$  (Cusil-

ABA<sup>®</sup>) [12, 13] and the (wt.%)  $\text{Ag}_{56}\text{Cu}_{42}\text{Ni}_2$  (AMS4765) [14]. In the present work, pseudo-alloys of the above compositions were composed by powder mixing. The wetting behaviour and the interfacial properties of those alloys in contact with different stainless steel alloys and with polycrystalline TZ-3Y were examined. As the surface energy of molten Ag is strongly related to the oxygen concentration, different atmospheric conditions were applied during the wetting experiments. Finally, as the long-term goal of this work is the implementation of those materials in the fuel cell technology, ageing experiments of the joints in the working conditions of a HDCFC were performed.

## Experimental procedure

Wetting properties and interfacial phenomena are the major factors controlling the effectiveness of joining different types of materials. An established method for studying the interfacial phenomena is that of a sessile drop of a liquid lying on the surface of a solid substrate (Fig. 1). In thermodynamic equilibrium the Young equation is valid:

$$\gamma_{sv} = \gamma_{sl} + \gamma_{lv} \cos \theta \quad (1)$$

where  $\gamma_{sv}$  and  $\gamma_{lv}$  are the surface energies of the solid substrate and the liquid phase respectively,  $\gamma_{sl}$  is the interfacial energy of solid–liquid and  $\theta$  is the contact angle. For a gas/liquid/solid system in equilibrium, the work of adhesion,  $w$ , i.e. the work required to separate an interface into two different free surfaces is given by the D upre equation:

$$w = \gamma_{sv} + \gamma_{lv} - \gamma_{sl} \quad (2)$$

Combining Eqs. (1) and (2) results in the Young–D upre equation:

$$w = \gamma_{lv}(1 + \cos \theta) \quad (3)$$

From Eq. (3) it is possible to determine the work of adhesion and so the strength of the bond between a liquid phase of known surface energy and a solid substrate only

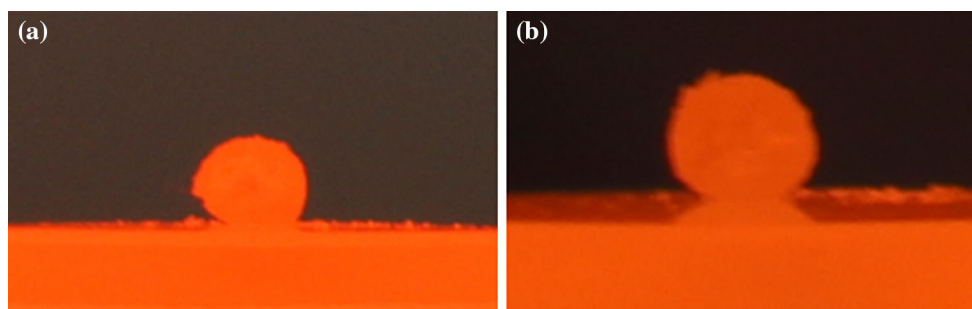


**Fig. 5** Wetting experiment of SS316L substrate in contact with liquid  $\text{Ag}_{63}\text{Cu}_{35.25}\text{Ti}_{1.75}$  at 1053 K in Ar/5 %H<sub>2</sub> (a) and with liquid  $\text{Ag}_{56}\text{Cu}_{42}\text{Ni}_2$  at 1313 K in vacuum (b)

by measuring the contact angle of the system. Also, as shown from Eq. (3), the work of adhesion is inversely proportional to the contact angle value, meaning that a low contact angle is essential for a sealing material.

For these reasons, the contact angle values of Ag and Ag-based alloys in contact with different substrates were measured. The wetting experiments were performed in a horizontal SiC resistance tube furnace in air, in vacuum and in flowing Ar/5 %H<sub>2</sub> atmosphere (80 ml/min). Quartz glass windows permitted the sideways in situ observation of the experiment using a digital camera. The contact angle value was measured by applying fitting of the Young–Laplace equation to sideways images of the drop captured by the digital camera, using the ImageJ image processing software. The equilibrium contact angle,  $\theta$ , for every temperature was established during the first minutes of the experiments and remained constant afterthought. During the wetting experiments, the temperature was monitored using an IR pyrometer.

For the wetting experiments, pure Ag (Alfa Aesar—purity 99.95 %) as well as Ag<sub>63</sub>Cu<sub>35.25</sub>Ti<sub>1.75</sub> and Ag<sub>56</sub>Cu<sub>42</sub>Ni<sub>2</sub> pseudo-alloys were used as liquid phase. The pseudo-alloys were composed by powder mixing metal powders of Ag (Alfa Aesar—99.9 % purity), Cu (Strem Chemicals—99.5 % purity), Ti (Alfa Aesar—99.5 % purity), and Ni (Sigma Aldrich—99 % purity). As substrates, different stainless steel alloys were selected. Initially, the austenitic stainless steel 316L which is a material that has been used in the scaling up of the HDCFC technology [15], mainly because of its low cost and high availability. Two other stainless steels, with the technical names Crofer22-APU and Crofer22H were also tested. Both these steels are

high-temperature ferritic stainless steels, developed jointly from ThyssenKrupp Nirosta GmbH and Forschungszentrum Jülich specifically for use in SOFCs, with the Crofer22H being an improved version of crofer22APU offering better creep properties. The composition for all the steels, according to their data sheets, is shown in Table 1. All steels were cut into round or square shape with 1.5–2.0 mm thickness. Powder of partially stabilized zirconia (TZ-3Y—Tosoh—99.8 % purity) was cold pressed into pellets of 10 mm diameters and ~3 mm thickness. The pellets were sintered for  $t = 20$  h at 1773 K to a final density 90 % of the theoretical. The Y<sub>2</sub>O<sub>3</sub> partially stabilized ZrO<sub>2</sub> with tetragonal precipitates was selected as insulation material for the good thermal shock resistance, high fracture toughness as well as resistance to wear and ageing it shows [16, 17] because of transformation toughening phenomena, resulting from the tetragonal to

**Fig. 7** Cross section SEM-EDX analysis on the interface of the system TZ-3Y/Ag<sub>56</sub>Cu<sub>42</sub>Ni<sub>2</sub> after wetting experiment at  $T = 1263$  K, in air

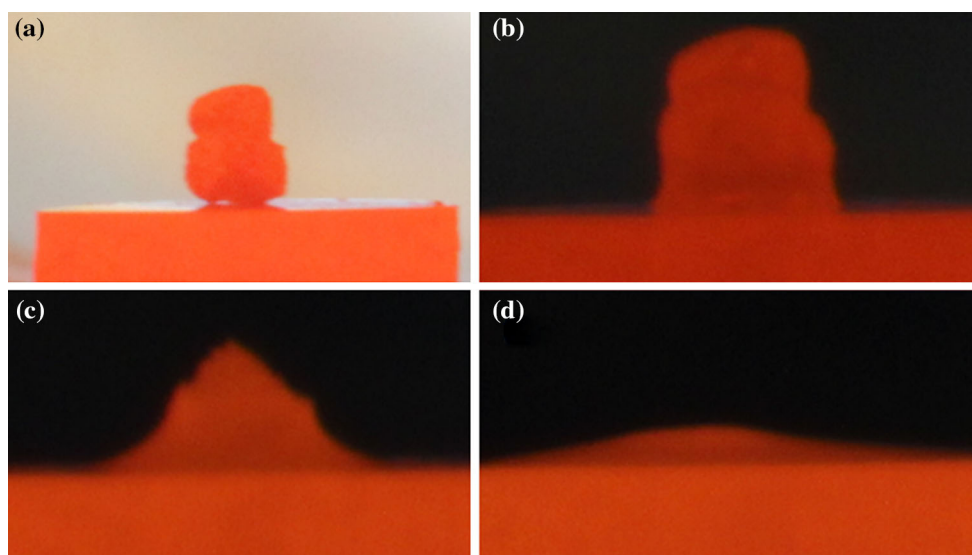
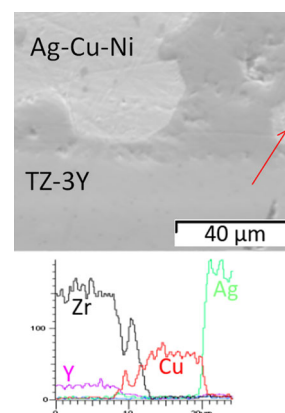


**Fig. 6** Temperature dependence of wetting on the system TZ-3Y/Ag<sub>56</sub>Cu<sub>42</sub>Ni<sub>2</sub> in air for  $T = 1198$  K (a),  $T = 1223$  K (b),  $T = 1258$  K (c) and  $T = 1263$  K (d)



monoclinic phase transformation [18]. All substrates were polished to a final roughness of 1  $\mu\text{m}$ .

## Results and discussion

### Pure Ag

Initially, wetting experiments in air with pure Ag in contact with the three steels and with TZ-3Y were performed. As shown in Table 2, all the systems are non-wetting with a

mean value of  $\theta = 90.9^\circ \pm 1.5^\circ$ ,  $\theta = 90.5^\circ \pm 1.4^\circ$ ,  $\theta = 108.7^\circ \pm 1.8^\circ$  for SS316L, Crofer22APU and Crofer22H, respectively, and  $\theta = 108.9^\circ \pm 0.9^\circ$  for TZ-3Y. In the case of the Ag/ferritic steels systems, the Ag drop is in contact with the protective  $\text{Cr}_2\text{O}_3$  protective layer that is formed in the surface of the Crofer steels and so a Ag/ceramic interface can be assumed. Because the melting temperature of Ag is above the recommended working temperature for continued use of the SS316L in oxidizing conditions (1193 K), during the wetting experiments a Fe–O rich layer is formed above the  $\text{Cr}_2\text{O}_3$  protective layer of

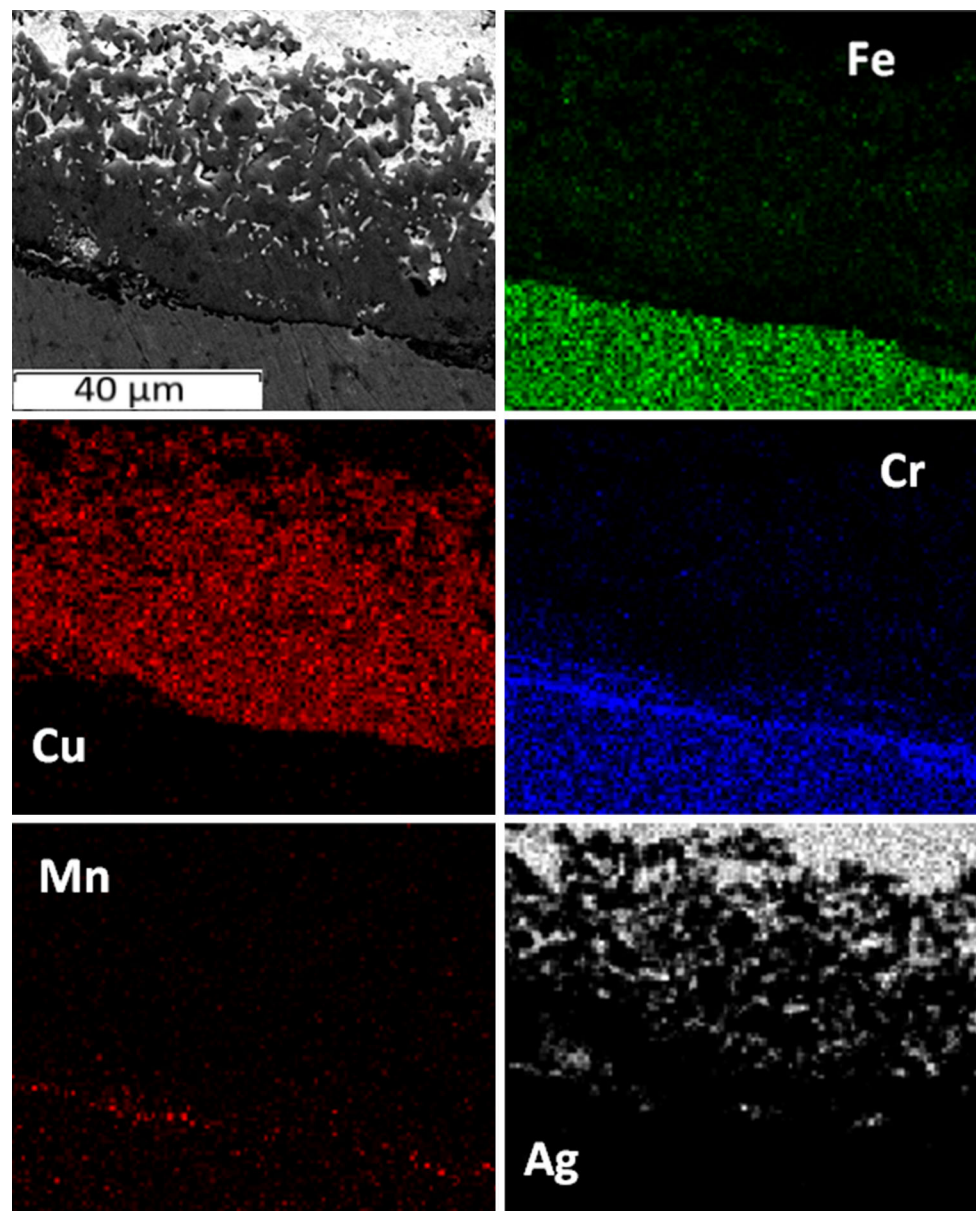


**Fig. 8** Cross section SEM-EDX mapping analysis on the interface of a Crofer22APU/ $\text{Ag}_{56}\text{Cu}_{42}\text{Ni}_2$  sample after wetting experiment at  $T = 1263\text{ K}$ , in air

the steel. Studies on austenitic steels with similar Cr concentration showed that the oxidation resistance of the steel is strongly related to the temperature and the amount of oxygen in the atmosphere. More specifically, in lower temperatures there is no significant effect of the atmosphere as the  $\text{Cr}_2\text{O}_3$  layer is always created and the Fe oxides are thermodynamically unstable. However, in higher temperatures and in high oxygen partial pressures,  $\text{Cr}_2\text{O}_3$  and Fe oxides can exist simultaneously and the growth of the oxides is controlled by kinetic factors. As the interdiffusion coefficients of Cr in the ferritic steels is about 10 times higher than in the austenitic steels, this Fe–O layer is not formed in the Crofer steels [19]. During the wetting experiment of SS316L by Ag, this very brittle Fe–O layer is formed, and as the systems cool down it causes the formation of cracks in the Ag–steel interface which leads to the complete separation of the droplet from the substrate.

The above systems in vacuum or in  $\text{Ar}/5\% \text{H}_2$  were not tested thoroughly as literature data for the wetting of ceramics by pure Ag in low oxygen concentrations reported very poor wettability ( $\theta > 100^\circ$ ) [8–11]. This non-wetting behaviour was confirmed after wetting experiments on the system Ag/Crofer22APU in  $\text{Ar}/5\% \text{H}_2$  and vacuum ( $P = 2.5 \times 10^{-3}$  mbar) at  $T = 1253$  K, with contact angle values of  $\theta = 121^\circ$  and  $\theta = 113^\circ$  respectively.

One way to improve the wettability of a noble metal is by adding an interface active compound which is also soluble in the metal. For the case of Ag, a material that fulfils these requirements is  $\text{CuO}_x$  as it forms a pseudo-binary alloy in solid state and is completely soluble in Ag in liquid state [20]. Addition of  $\text{CuO}_x$  is very effective in reducing the contact angle values. Wetting experiments found in the literature for systems of Ag–CuO pseudo-alloys in contact with ceramic and steel substrates showed very good wettability ( $\theta < 20^\circ$ ) [21–24]. A cost-effective way of introducing the  $\text{CuO}_x$  in the Ag is the deposition of a thin layer of Cu on the surface of the substrate that is later oxidized to  $\text{CuO}_x$ . During the wetting experiment, the  $\text{CuO}_x$  is dissolved in the liquid Ag that results in a much lower contact angle compared to the pure Ag [25]. For this study, a thin layer ( $\approx 0.3 \mu\text{m}$ ) of Cu was deposited on the substrates using evaporation coating in vacuum ( $3 \times 10^{-5}$  mbar), and wetting experiments with liquid Ag in air were performed. For the steel substrates and for  $T = 1253$  K, the contact angles values measured in this case were  $\theta = 83.8^\circ$  for the system SS316L/CuO/Ag,  $\theta = 55.1^\circ$  for the system Crofer22APU/CuO/Ag and  $\theta = 58.3^\circ$  for the system Crofer22H/CuO/Ag. For both the ferritic steels, the contact angle in this case is significant reduced compared with the experiments using only pure Ag. For the system Crofer22APU/CuO/Ag, the measured contact angles are in agreement with data found in the literature [25].

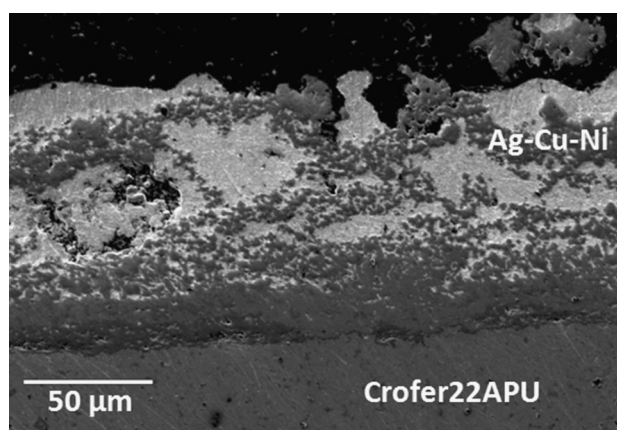


**Fig. 9** SEM image of the surface of the drop for the system Crofer22APU/Ag<sub>56</sub>Cu<sub>42</sub>Ni<sub>2</sub> after wetting experiment at  $T = 1263$  K, in air

Cross section SEM images of the interface on the Crofer22H/CuO/Ag system showed the existence on a thin ( $\approx 2 \mu\text{m}$ ) reaction zone that penetrates in the silver. SEM-EDX analysis on the interface showed that this reaction zone is consisted of Cr-rich oxides (Fig. 2a). Similar results were obtained for the Crofer22APU/CuO/Ag system. In the case of SS316L, the contact angle is slightly reduced. Also, as in the case of pure Ag in contact with SS316L, a Fe–O brittle layer ( $\approx 8 \mu\text{m}$ ) was formed on the interface (Fig. 2b) that reduces the stability of the bond, as in some cases this Fe–O layer is detached from the surface of the steel and can be found on the Ag drop (Fig. 3). In order to deal with this problem, on the surface of the SS316L samples, a thin ( $\approx 0.3 \mu\text{m}$ ) layer of Ti was deposited and then the samples were treated at 773 K for  $t = 5$  h in air. In these conditions, the Ti layer will oxidize and react with the  $\text{Cr}_2\text{O}_3$  layer on the surface of the steel to form Titanium-substituted chromium oxides (CTO), with the general formulation  $\text{Cr}_{2-x}\text{Ti}_x\text{O}_{3+y}$  [26, 27], that will protect the surface of the steel from oxidation. After that, a Cu layer was deposited as before and wetting experiment with Ag was performed. The contact angle in this case was slightly lower than before with a value of  $\theta = 81.1^\circ$ . Although the wettability did not change a lot, cross section SEM-EDX analysis on the interface showed that in this case the reaction zone and the Fe–O layer is reduced from  $\sim 8$  to  $\sim 3 \mu\text{m}$  (Fig. 4). Because of this, the stability of the bond was increased and no separation of the two phases occurred. In any case because, as mentioned earlier, the melting point of pure Ag is above the recommended working temperature for continued use of the SS316L in oxidizing conditions, a sealing material with lower melting point or with good wetting properties in protective atmosphere would be preferable for use with this steel.

### Ag–Cu–Ti

The (wt.%)  $\text{Ag}_{63}\text{Cu}_{35.25}\text{Ti}_{1.75}$  pseudo-alloy was composed by powder mixing the pure metal powders. A sealing alloy with the same composition has been developed from Morgan Advanced Materials with the commercial name Cusil-ABA. In order to test the possible use of this pseudo-alloy as sealing material, wetting experiments in contact with steel and TZ-3Y substrates were performed. Because of the presence of the Ti in the pseudo-alloy and its fast oxidation ( $\Delta G_{(\text{TiO}_2)_{(900)}} = -732.128 \text{ kJ}$ ), the experiments

were performed only in flowing  $\text{Ar}/5\% \text{H}_2$  atmosphere (80 ml/min) and in vacuum ( $2.5 \times 10^{-3} \text{ mbar}$ ).

In reducing conditions, the surface of the steel will not form this Fe–O layer at high temperatures, and moreover the liquidus temperature for the pseudo-alloy (1023 K) is much lower than the melting point of pure Ag (1235 K). However, the pseudo-alloy showed very poor wettability with all the substrates with  $\theta > 110^\circ$  (Fig. 5a). In reducing conditions Cu and Ti will not form the corresponding oxides and so the three metals will mix into a ternary liquid solution. The droplet showed no adhesion to the

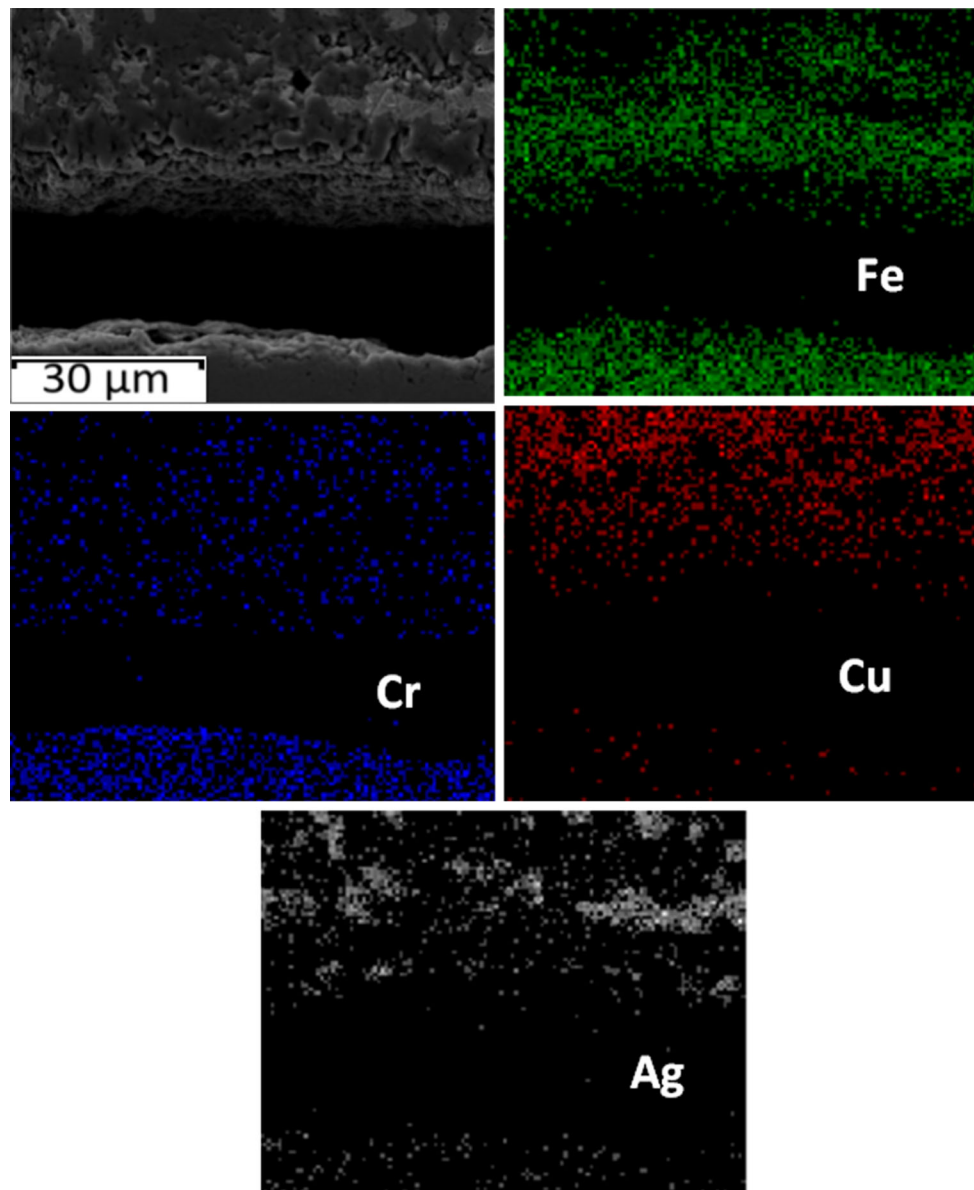


**Fig. 10** Cross section SEM-EDX mapping analysis on the interface of a SS316L/ $\text{Ag}_{56}\text{Cu}_{42}\text{Ni}_2$  system after wetting experiment at  $T = 1263 \text{ K}$ , in air



substrates, and after the cool down it detached the substrate.

Wetting experiments with steel and TZ-3Y substrates were performed also in vacuum ( $P = 2.5 \times 10^{-3}$  mbar). At these conditions, the liquidus temperature of the alloy is higher (1093 K) than in Ar/5 %H<sub>2</sub> but again lower than the melting point of pure Ag. The contact angles for all the systems in this case were significantly lower than before, with a mean value of  $\theta \approx 40^\circ$  for the steels and  $\theta \approx 50^\circ$  for the polycrystalline TZ-3Y. The values for the steels are higher than literature data for the wetting of SS316 substrates by the Cusil-ABA alloy [28] but are in agreement with data obtained for systems of ceramic substrates in contact with liquid pseudo-alloys of similar compositions [29, 30]. The improvement in the wettability caused by the addition of the Ti compared to the Ag:CuO<sub>x</sub> system is due to a two step modification of the interface. Initially the interface active Ti migrates towards the liquid/solid interface. Secondly, a thin Ti oxide layer is formed on the solid side of the interface [31] and because of its very low surface energy ( $\gamma_{sv}(\text{TiO}_2) = 0.800 - 0.167 \times 10^{-3} T$  [32]) the contact angle values reduced significantly.

### Ag–Cu–Ni

A pseudo-alloy with the composition (wt.% Ag<sub>56</sub>Cu<sub>42</sub>Ni<sub>2</sub>) was prepared. An alloy of this composition is typically used for joining ferrous metals and steels. Initially, wetting experiments with steel and TZ-3Y substrates in vacuum ( $P = 2.5 \times 10^{-3}$  mbar) showed very poor wettability with contact angle values  $\theta \approx 140^\circ$  for the SS316L (Fig. 5b),  $\theta \approx 120^\circ$  for the two Crofer steels and  $\theta \approx 135^\circ$  for the TZ-3Y. The liquidus temperature for this pseudo-alloy in these conditions was  $T = 1153$  K. Although this temperature is very close to the highest recommended working temperature of the SS316L, the absence of oxygen protects the surface of the steel and no Fe–O layer is formed. However, because of the very high contact angles, there is almost no adhesion between the alloy and the substrates and after the cool down the droplet detaches the substrate. The reason for this non-wetting behaviour is that the oxidation of Cu ( $\Delta G_{(\text{CuO})_{(900)}} = -51.822$  kJ) and Ni ( $\Delta G_{(\text{NiO})_{(900)}} = -133.576$  kJ in air) is not possible in this conditions and so, as in the case of the Ag<sub>63</sub>Cu<sub>35.25</sub>Ti<sub>1.75</sub> in Ar/5 %H<sub>2</sub>, the three metals will form a ternary liquid solution. For the same reason, similar non-wetting behaviour was observed in reducing conditions (Ar/5 %H<sub>2</sub>). A layer that can be observed on the surface of the drop is believed to be because of the diffusion of the Cr and Fe from the surface of the steel into the liquid phase and the formation of a Fe–Cr alloy [25].

In the wetting experiments carried out in air, the results were completely different. The pseudo-alloy showed

excellent wetting with all the steels and with the TZ-3Y substrates. As shown in Fig. 6, after the initial oxidation of the pseudo-alloy, at temperatures above the liquidus temperature ( $T = 1263$  K) the alloy immediately spreads on the surface of the ceramic ( $\theta < 10^\circ$ ). SEM-EDX analysis on the TZ-3Y/Ag<sub>56</sub>Cu<sub>42</sub>Ni<sub>2</sub> interface did not show any reaction zone, only a  $\sim 10$   $\mu\text{m}$  Cu oxide layer is formed on the interface (Fig. 7), as the CuO<sub>x</sub> is very interfacial active and trends to migrate towards the interface. Wetting experiments with steel substrates showed similar wettability ( $\theta < 10^\circ$ ). The SEM-EDX analysis for experiments with Crofer22APU substrate revealed the formation of a Mn–Cr layer on the steel side of the interface (Fig. 8). The grain boundary diffusion coefficients for the Mn, Cr and Fe ions of the steel through the Cr<sub>2</sub>O<sub>3</sub> layer are in the order  $D_{\text{gb}}(\text{Fe}) < D_{\text{gb}}(\text{Cr}) < D_{\text{gb}}(\text{Mn})$  [33] and so the faster diffused Mn migrate towards the interface reacting with the Cr. This Cr–Mn reaction zone acts as stabilizer to the Cr–O protective layer of the steel and increases the oxidation resistance of the steel [19]. Diffusion of Cr and Fe in the liquid phase created inclusions of a Fe–Cr alloy that can be found in the interface but also inside the droplet (Fig. 9). Similar results were revealed for the Crofer22H substrate.

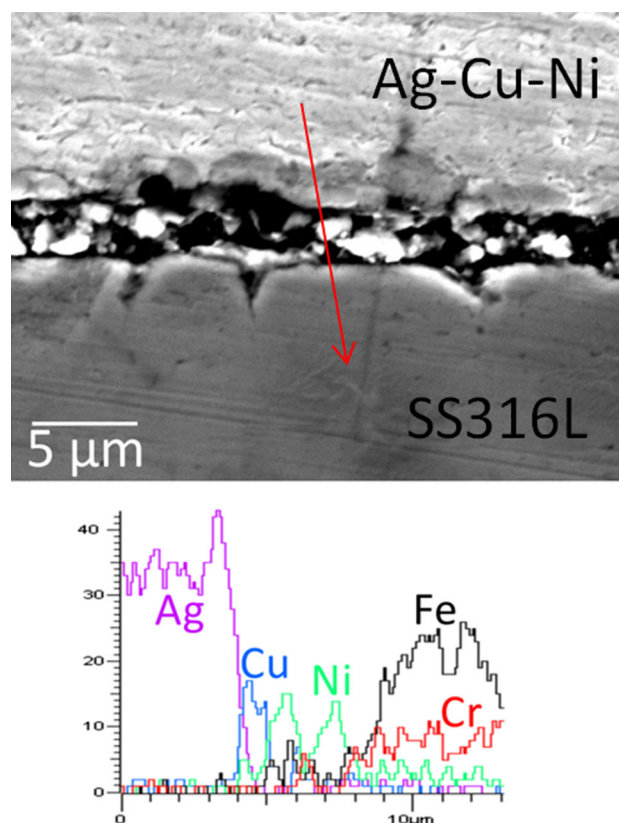


**Fig. 11** Cross section SEM-EDX line scanning analysis on the interface of a SS316L/Ag<sub>56</sub>Cu<sub>42</sub>Ni<sub>2</sub> system after wetting experiment at  $T = 1093$  K, in low vacuum ( $P = 1.5 \times 10^{-1}$  mbar)



In both steels, despite the reactions happening in the interface, the pseudo-alloy showed excellent adhesion with the substrates, as no cracks or separation were observed. Because the liquidus temperature of the pseudo-alloy is very high, in the experiment with SS316L the pseudo-alloy reacts with the brittle Fe–O rich layer that forms on the surface of the steel. During the cooling down, this layer will crack and completely detached from the steel (Fig. 10).

As this pseudo-alloy shows better wettability with the presence of oxygen but the surface of the SS316L is rapidly

oxidized in air, wetting experiments in low vacuum ( $P = 1.5 \times 10^{-1}$  mbar) were performed. In these conditions the wettability of the steel by the pseudo-alloy was improved compared with using higher vacuum, with  $\theta \approx 65^\circ$  at the liquidus temperature of the pseudo-alloy ( $T = 1093$  K). As detected with SEM-EDX analysis on the interface (Fig. 11), in this case a Fe–Ni phase is formed in the interface. The interface active Cu of the pseudo-alloy migrates towards the interface and creates a thin layer over the Fe–Ni phase. A layer of Fe–O follows on the steel surface and although this layer is much thinner than the one

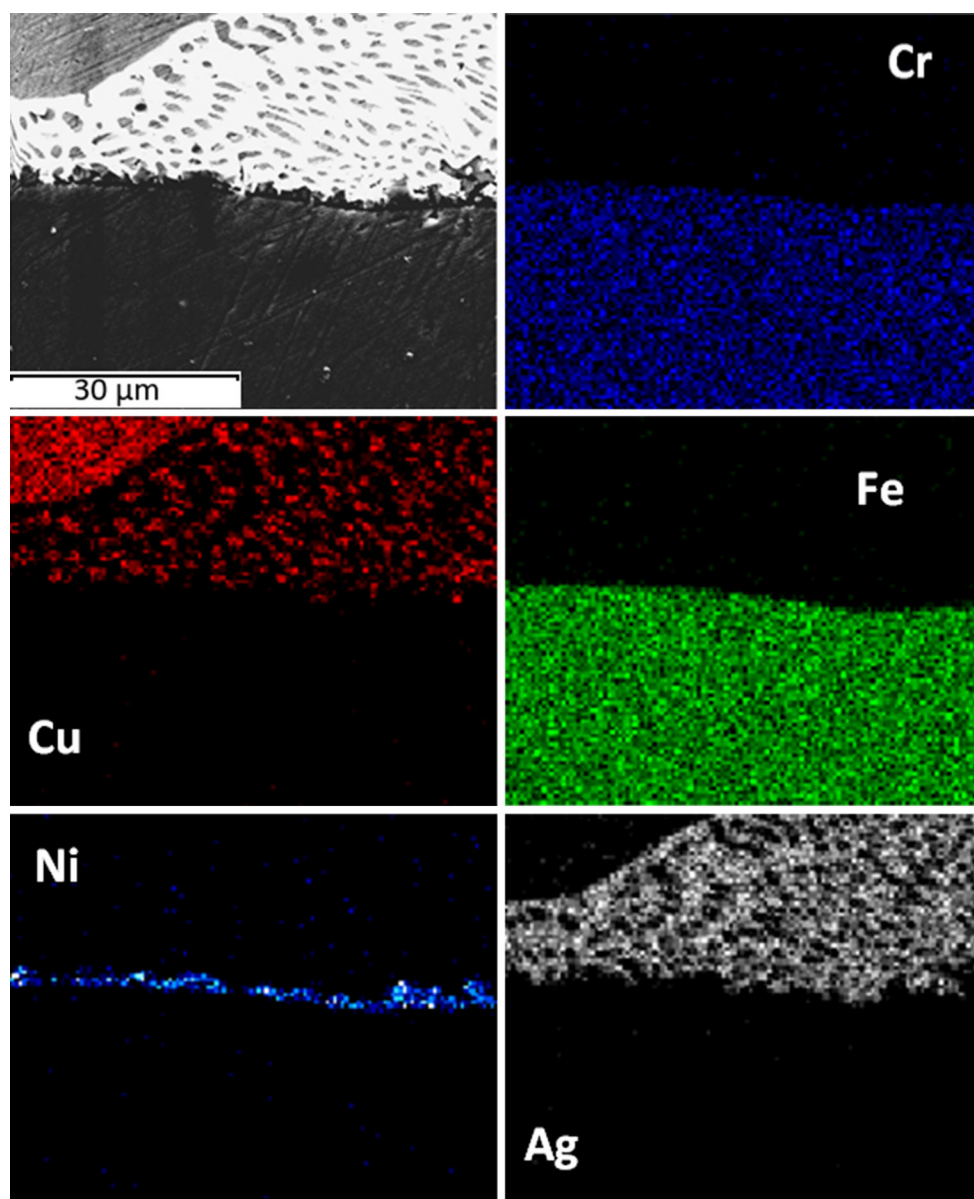


**Fig. 12** Cross section SEM-EDX mapping analysis on the interface of a Crofer22APU/Ag<sub>56</sub>Cu<sub>42</sub>Ni<sub>2</sub> system after wetting experiment at  $T = 1263$  K, in low vacuum ( $P = 1.5 \times 10^{-1}$  mbar)

created in air, during the cooling down, some cracks are formed and the droplet in some cases separates from the substrate. However, the possible use of the  $\text{Ag}_{56}\text{Cu}_{42}\text{Ni}_2$  pseudo-alloy as sealing material for SS316L in controlled vacuum conditions can be investigated in the future. For comparison reasons, the system Crofer22APU/ $\text{Ag}_{56}\text{Cu}_{42}\text{Ni}_2$  was also examined. The contact angle in this case is increased ( $\theta \approx 74^\circ$ ) but the SEM-EDX analysis showed the absence of any reaction zone in the interface. The Ni from the pseudo-alloy is found to migrate in the interface and the diffusion of Cr and Fe in the droplet does not occur in these conditions (Fig. 12).

### Heat treatment of the pseudo-alloys

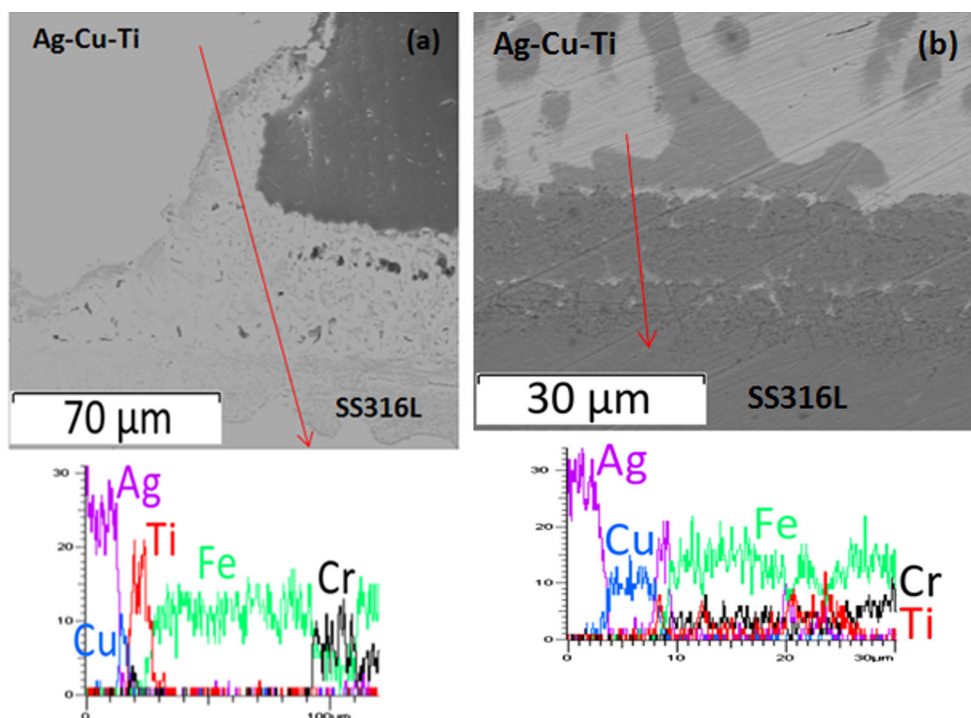
Selected systems that showed satisfactory results were tested and aged in the working conditions of a HDCFC. Specifically, samples with the pseudo-alloys  $\text{Ag}_{63}\text{Cu}_{35.25}\text{Ti}_{1.75}$  in contact with SS316L and with Crofer22H in vacuum ( $P = 2.5 \times 10^{-3}$  mbar) at  $T = 1100$  K as well as a “sandwich” of Crofer22H/ $\text{Ag}_{56}\text{Cu}_{42}\text{Ni}_2$ /TZ-3Y in air at  $T = 1263$  K were prepared. All these samples were later treated for  $t = 120$  h at  $T = 1023$  K in  $\text{CO}_2$  atmosphere, conditions similar to the working conditions of the HDCFC, in order to evaluate the stability of the sealants and the steels.

In the case of the system SS316L/ $\text{Ag}_{63}\text{Cu}_{35.25}\text{Ti}_{1.75}$  in vacuum, SEM-EDX analysis showed that after 120 h in the

working temperature of a HDCFC a thick ( $\approx 70$   $\mu\text{m}$ ) Fe–O layer was created on the free surface of the steel, followed by a much thinner  $\text{Cr}_2\text{O}_3$  layer and also that the surface of the droplet is covered by a Ti oxide layer (Fig. 13a). In the steel-sealant interface, although the Fe–O layer is significantly reduced ( $\approx 20$   $\mu\text{m}$ ) it is found to be detached from the steel with a thin Ti layer found on the steel side of the interface and a Cu layer on the other side of the detached Fe–O. Inside the droplet the rest of the Cu forms Cu-rich agglomerates (Fig. 13b). For the system Crofer22H/ $\text{Ag}_{63}\text{Cu}_{35.25}\text{Ti}_{1.75}$ , SEM-EDX analysis revealed that although a Fe-rich layer is not formed, a much thinner ( $<5$   $\mu\text{m}$ ) Cr–Fe layer is detached from the surface of the steel into the droplet (Fig. 14). Ti concentration is high in both sides of the detached layer and Cu agglomerates can be found inside the droplet. The detachment of the surface of the steel in both SS316L and Crofer22H substrate indicates possible Fe–Cr–Ti reactions that have to be investigated in the future.

In the case of Crofer22H in contact with  $\text{Ag}_{56}\text{Cu}_{42}\text{Ni}_2$ , the SEM-EDX analysis after the heat treatment showed the formation of a very thick ( $>30$   $\mu\text{m}$ ) reaction zone. As shown before (Fig. 8), during the wetting experiment a Cu-rich zone is formed in the interface. After the heat treatment, this Cu zone reacts with the Cr and Fe ions that are slowly diffused from the steel to the droplet, creating a Cu–Fe–Cr–O layer on the interface, followed by a Cu–Fe–O layer (Fig. 15a). This comes in agreement with literature

**Fig. 13** Cross section SEM-EDX mapping analysis on the interface of a SS316L/ $\text{Ag}_{63}\text{Cu}_{35.25}\text{Ti}_{1.75}$  system after wetting experiment at  $T = 1100$  K, in vacuum ( $P = 2.5 \times 10^{-3}$  mbar) and heat treatment for  $t = 120$  h at  $T = 1023$  K in  $\text{CO}_2$  atmosphere



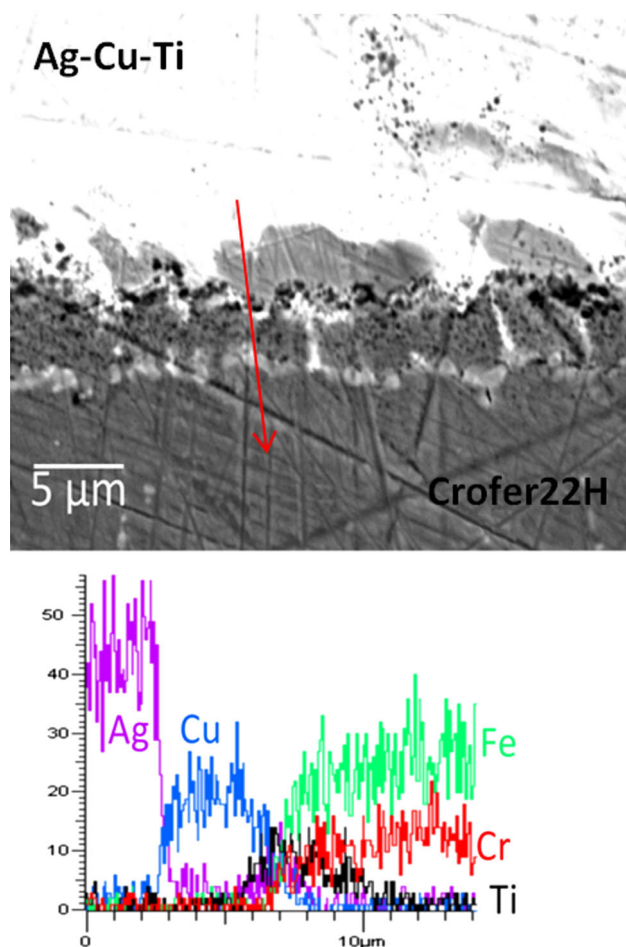


**Fig. 14** Cross section SEM-EDX mapping analysis on the interface of a Crofer22H/Ag<sub>63</sub>Cu<sub>35.25</sub>Ti<sub>1.75</sub> system after wetting experiment at  $T = 1100$  K, in vacuum ( $P = 2.5 \times 10^{-3}$  mbar) and heat treatment for  $t = 120$  h at  $T = 1023$  K in CO<sub>2</sub> atmosphere

data for Crofer22APU in contact with Ag–CuO pseudo-alloys [25]. No cracks or detachment of this layer from the surface of the steel were observed as in the case of steels in contact with the Ag<sub>63</sub>Cu<sub>35.25</sub>Ti<sub>1.75</sub>. For the system TZ-3Y/Ag<sub>56</sub>Cu<sub>42</sub>Ni<sub>2</sub>, the SEM-EDX analysis showed only the presence of Ag in the interface, as the Cu has migrated towards the Crofer22H/Ag<sub>56</sub>Cu<sub>42</sub>Ni<sub>2</sub> of the sandwich (Fig. 15b) and that no reactions occurred between the two phases.

## Conclusion

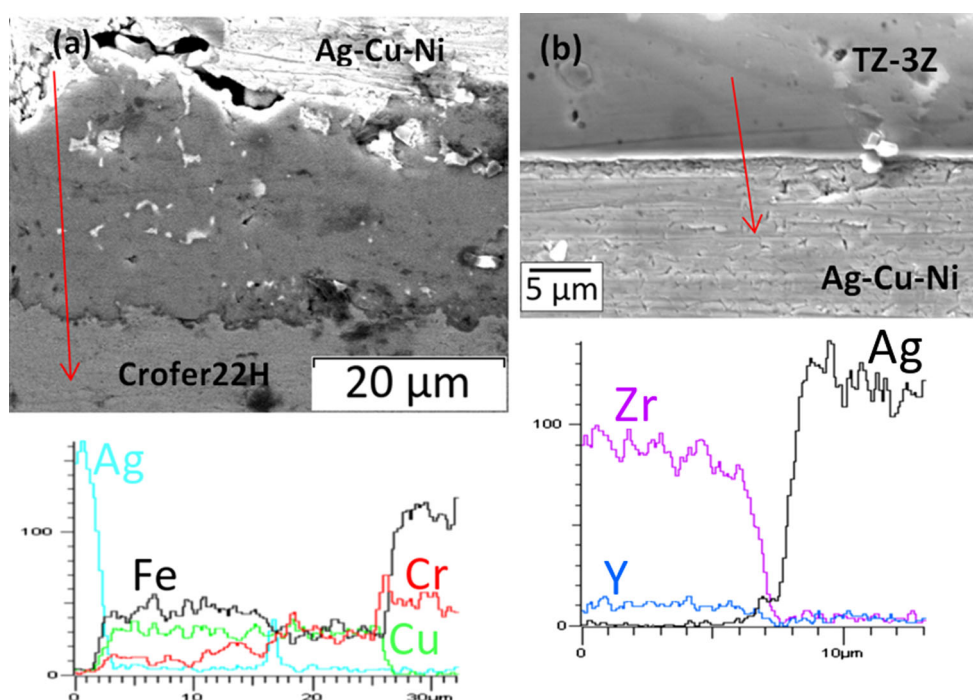
Ag as well as Ag–Cu–Ti and Ag–Cu–Ni pseudo-alloys were examined as possible sealing materials for use in the HDCFC technology. Wetting experiments of the above

materials in contact with austenitic and ferritic steels and with polycrystalline TZ-3Y were performed in order to evaluate the interfacial properties of the above systems in different atmospheric conditions. Pure Ag showed poor wettability with all the substrates. In order to lower the contact angle values, the interfacial active CuO<sub>x</sub> was introduced to the systems, by depositing a thin layer of Cu in the surface of the substrate. This improved the wettability and so the adhesion between the two phases but in the case of the austenitic steel SS316L the melting point of pure Ag is higher than its recommended working temperature and a brittle Fe oxide is formed on its surface. The deposition of a Ti layer on the surface of the steel improved its oxidation resistance but again the Fe oxide was formed, reducing the stability of the joint. As the wetting properties of pure Ag in low oxygen concentrations are very poor, two Ag-based pseudo-alloys were tested. The Ag<sub>63</sub>Cu<sub>35.25</sub>Ti<sub>1.75</sub> pseudo-alloy used in vacuum ( $P = 2.5 \times 10^{-3}$  mbar) showed improved wettability with all the substrates but after heat treatment for 120 h in the operating conditions of a HDCFC ( $T = 1023$  K, CO<sub>2</sub> atmosphere) SEM-EDX analysis revealed the formation of a reaction zone that detached from the surface of both the austenitic and ferritic steel tested. The Ag<sub>56</sub>Cu<sub>42</sub>Ni<sub>2</sub> pseudo-alloy was also tested in air and in low vacuum ( $P = 1.5 \times 10^{-1}$  mbar). In air it showed excellent wettability with all the substrates ( $\theta < 10^\circ$ ) but its high liquidus temperature make it unsuitable for use with SS316L. In low vacuum the contact angles for the system SS316L/Ag<sub>56</sub>Cu<sub>42</sub>Ni<sub>2</sub> were increased but in these low oxygen concentrations the formation of the Fe oxide on the surface of the steel was limited. After heat treatment of an air brazed TZ-3Y/Ag<sub>56</sub>Cu<sub>42</sub>Ni<sub>2</sub>/Crofer22H “sandwich” in the above conditions, SEM-EDX analysis showed the migration of the Cu towards the steel/Ag<sub>56</sub>Cu<sub>42</sub>Ni<sub>2</sub> interface and the formation of a thick Cu–Fe–Cr–O reaction zone and also the absence of reactions on the ceramic/Ag<sub>56</sub>Cu<sub>42</sub>Ni<sub>2</sub> interface. In any case, for both the pseudo-alloys after the heat treatment and despite the reactions occurred on the steel/pseudo-alloy interfaces, the two phases did not separate.

The austenitic SS316L showed limited resistance to oxidation in high temperatures. A brittle Fe–O layer is formed on the surface of the steel above the Cr–O protective layer. This not only affected the mechanical stability but also may reduce the electrical conductivity of the steel, as the Fe–O<sub>x</sub> is less conductive than the Cr–O. On the other hand, both crofer22APU and crofer22H ferritic steel shown good oxidation resistance in high temperatures in air. The Mn found to migrate towards the surface and to stabilize the Cr–O protective layer.



**Fig. 15** Cross section SEM-EDX mapping analysis on the interface of the Crofer22H/Ag<sub>56</sub>Cu<sub>42</sub>Ni<sub>2</sub> (a) and TZ-3Y/Ag<sub>56</sub>Cu<sub>42</sub>Ni<sub>2</sub> (b) systems after wetting experiment at  $T = 1263$  K, in air and heat treatment for  $t = 120$  h at  $T = 1023$  K in CO<sub>2</sub> atmosphere



**Acknowledgements** The authors would like acknowledge the financial support received from the Engineering and Physical Sciences Research Council [EP/K015540/1] and the European Coal and Steel Community [RFCR-CT-2011-00004]. The research data supporting this publication can be accessed at <http://dx.doi.org/10.17630/557f671e-8881-4b9d-8c11-a8d21de1dc3d>.

#### Compliance with ethical standards

**Conflict of interest** The authors declare that they have no conflict of interest.

**Open Access** This article is distributed under the terms of the Creative Commons Attribution 4.0 International License (<http://creativecommons.org/licenses/by/4.0/>), which permits unrestricted use, distribution, and reproduction in any medium, provided you give appropriate credit to the original author(s) and the source, provide a link to the Creative Commons license, and indicate if changes were made.

## References

- Giddey S, Badwal SPS, Kulkarni A, Munnings C (2012) A comprehensive review of direct carbon fuel cell technology. *Prog Energy Comb Sci* 38:360–399
- Deleebeeck L, Hansen KK (2014) Hybrid direct carbon fuel cells and their reaction mechanisms a review. *J Solid State Electrochem* 18:861–882
- Menzler HH, Tietz F, Uhlenbruck S, Buchkremer HP, Stöver D (2010) Materials and manufacturing technologies for solid oxide fuel cells. *J Mater Sci* 45:3109–3135. doi:10.1007/s10853-010-4279-9
- Mahapatra MK, Lu K (2010) Seal glass for solid oxide fuel cells. *J Power Sources* 195:7129–7139
- Chang HT, Lin CK, Liu CK (2010) Effects of crystallization on the high-temperature mechanical properties of a glass sealant for solid oxide fuel cell. *J Power Sources* 195:3159–3165
- Szabo P, Arnold J, Franc T, Gindrat M, Refke A, Zagst A, Ansar A (2009) Progress in the metal supported solid oxide fuel cells and stacks for APU. *ECS Trans* 25(2):175–185
- Lamp P, Tachtler J, Finkenwirth O, Mukerjee S, Shaffer S (2013) Development of an auxiliary power unit with solid oxide fuel cells for automotive applications. *Fuel Cells* 3:146–152
- Nogi K, Oishi K, Ogino K (1989) Wettability of solid oxides by liquid pure metals. *Mater Trans JIM* 30:137–145
- Ueki M, Naka M, Okamoto I (1986) Wettability of some metals against zirconia ceramics. *J Mater Sci Lett* 5:1261–1262
- Mehrotra SP, Chaklader ACD (1985) Interfacial phenomena between molten metals and sapphire substrate. *Metall Trans B* 16:567–575
- Chatain D, Chabert F, Ghetta V, Fouletier J (1994) New experimental setup for wettability characterization under monitored oxygen activity: II, wettability of sapphire by silver-oxygen melts. *J Am Ceram Soc* 77:197–201
- Singh M, Matsunaga T, Lin HT, Asthana R, Ishikawa T (2012) Microstructure and mechanical properties of joints in sintered SiC fiber-bonded ceramics brazed with Ag–Cu–Ti alloy. *Mater Sci Eng A* 557:69–76
- Kobsiriphat W, Barnett S (2008) Ag–Cu–Ti braze materials for sealing SOFCs. *J Fuel Cell Sci Technol* 5:011002
- Landingham RL, Shell TE (1987) Steel bonded dense silicon nitride compositions and method for their fabrication. US 4703884 A, 3 Nov 1987
- Chien AC, Corre G, Antunes R, Irvine JTS (2013) Scaling up of the hybrid direct carbon fuel cell technology. *Int J Hydrog Energy* 38:8497–8502
- Kondoh J, Shiota H, Kawachi K, Nakatani T (2004) Yttria concentration dependence of tensile strength in yttria-stabilized Zirconia. *J Alloys Compd* 365:253–258
- Timakul P, Jinawath S, Aungkavattana P (2008) Fabrication of electrolyte materials for solid oxide fuel cells by tape-casting. *Ceram Int* 34:867–871



18. Hannink RHJ, Kelly PM, Muddle BC (2000) Transformation toughening in zirconia-containing ceramics. *J Am Chem Soc* 83:461–487
19. Sabioni ACS, Huntz AM, Luz ECD, Mantel M, Haut C (2003) Comparative study of high temperature oxidation behaviour in AISI 304 and AISI 439 stainless steels. *Mater Res* 6:179–185
20. Shao ZB, Liu KR, Liu LQ, Liu HK, Dou SX (1993) Equilibrium phase diagrams in the systems PbO–Ag and CuO–Ag. *J Am Ceram Soc* 76:2663–2664
21. Weil KS, Coyle CA, Hardy JS, Kim JY, Xia GG (2004) Alternative planar SOFC sealing concepts. *Fuel Cells Bull* 5:11–16
22. Meier AM, Chidambaram PR, Edwards GR (1995) A comparison of the wettability of copper–copper oxide and silver–copper oxide on polycrystalline alumina. *J Mater Sci* 30:4781–4786. doi:[10.1007/BF01154485](https://doi.org/10.1007/BF01154485)
23. Weil KS, Kim JY, Hardy JS (2005) Reactive air brazing: a novel method of sealing SOFCs and other solid-state electrochemical devices. *Electrochem Solid State Lett* 8:A133–A136
24. Kim JY, Hardy JS, Weil KS (2005) Effects of CuO content on the wetting behavior and mechanical properties of a Ag–CuO braze for ceramic joining. *J Am Ceram Soc* 88:2521–2527
25. Chatzimichail R, Triantafyllou G, Tietz F, Nikolopoulos P (2014) Interfacial properties of (Ag + CuO) brazes used as sealing materials in SOFC stacks. *J Mater Sci* 49:300–313. doi:[10.1007/s10853-013-7706-x](https://doi.org/10.1007/s10853-013-7706-x)
26. Henshaw GS, Dawson DH, Williams DE (1995) Selectivity and composition dependence of response of gas-sensitive resistors. *J Mater Chem* 5:1791–1800
27. Williams DE (1999) Semiconducting oxides as gas-sensitive resistors. *Sens Actuators B* 57:1–16
28. Abed A, Jalham IS, Hendry A (2001) Wetting and reaction between  $\beta'$ -sialon, stainless steel and Cu–Ag brazing alloys containing Ti. *J Eur Ceram Soc* 21:283–290
29. Nicholas MG, Mortimer DA, Jones LM, Crispin RM (1990) Some observations on the wetting and bonding of nitride ceramics. *J Mater Sci* 25:2679–2689. doi:[10.1007/BF00584866](https://doi.org/10.1007/BF00584866)
30. Voytovych R, Ljungberg LY, Eustathopoulos N (2004) The role of adsorption and reaction in wetting in the CuAg–Ti/alumina system. *Scr Mater* 51:431–435
31. Kritsalis P, Coudurier L, Eustathopoulos N (1991) Contribution to the study of reactive wetting in the CuTi/Al<sub>2</sub>O<sub>3</sub> system. *J Mater Sci* 26:3400–3408. doi:[10.1007/BF01124693](https://doi.org/10.1007/BF01124693)
32. Bruce RH (1965) *Science of ceramics*, vol 12. Academic Press, London
33. Sabioni ACS, Huntz AM, Borges LC, Jomard F (2007) First study of manganese diffusion in Cr<sub>2</sub>O<sub>3</sub> polycrystals and thin films by SIMS. *Philos Mag* 87:1921–1937